Pull-out tests on bituminous specimens with steel wire mesh reinforcements

Conference Paper · June 2016

DOI: 10.1201/9781315643274-98

6 authors, including:

Francesco Mazzotta
University of Bologna

Andrea Simone
University of Bologna

Valeria Vignali
University of Bologna

Claudio Lantieri
University of Bologna

Functional Pavement Design – Erkens et al. (Eds)
© 2016 Taylor & Francis Group, London, ISBN 978-1-138-02924-8

Pull-out tests on bituminous specimens with steel wire mesh reinforcements

F. Mazzotta, A. Simone, V. Vignali, C. Lantieri, C. Sangiorgi & G. Dondi
Department of Civil, Chemical, Environmental and Materials Engineering, University of Bologna, Italy

ABSTRACT: Steel reinforcements within the asphalt pavement layers have widely demonstrated to be a successful technology to avoid the propagation of bottom-up fatigue cracks. However, the tensile stresses, induced by heavy vehicles at the bottom of bound layers, induce the crossbars unthreading compromising their proper functioning. In addition, the high temperature during laying produces dilatations of the steel reinforcement.

The main topic of this paper is the study of the asphalt layer—steel reinforcement system, analyzing the mechanical behavior and the construction materials optimization. Pull-out tests were carried out to evaluate the effects of three different crossbars steel reinforcement in terms of pull-out resistance. The reinforcement shape and the coating materials influence the behavior of the steel wire mesh and its interaction with the asphalt mixture.

1 INTRODUCTION

Geosynthetics have been widely used as reinforcement in structures with unbound materials, such as pavements, slopes, retaining walls and embankments. It has been shown that, in a pavement system, the inclusion of geosynthetics can significantly improve the pavement performance (Xiaochao et al. 2008, Tataranni et al. 2015). They influence, in fact, the aggregate contact and interlocking, which control the load-bearing and load-transferring capability of asphalt pavements (Dondi et al. 2012, 2014). A lot of studies have shown that the presence of steel geosynthetics reinforcement at the bottom of asphalt layers should reduce the principal stresses and the vertical deformations, thus increasing the bearing capacity and service life. In particular the steel mesh provides a decrease of the tensile strain at the bottom of the asphalt mixture, hindering the initiation and propagation of bottom-up cracking (Said et al. 2009, Namir et al. 2013). Vicari (2007) presents an overview of the main results obtained from researches carried out by Universities around the world on pavements reinforced with a steel mesh, in terms of improvement of the fatigue life. This study shows that in all cases the pavement fatigue life increases more than 50%. Baek and Al-Qadi (2006) evaluated the role of a single steel reinforcement wire in a two layered beam specimen on delaying crack development by numerical analysis. The crack initiation time was delayed and the growth rate decreased since the steel reinforcement held and redistributed concentrated stresses around a crack tip. They mentioned that the role of the steel reinforcement was affected by the interface conditions, the HMA material properties and the temperature. Bondt and Scarpas (2006) studied whether the shape and the bond of the reinforcement can influence the behavior of these products inside the superstructures. Overseas experience has indicated that the placement/construction procedures and the field conditions can strongly influence the field performance of reinforcement products. Defects in a reinforced asphalt overlay due to installation and construction problems (e.g. bonding between pavement layers, bulging of the reinforcing material, etc.) may significantly reduce the effectiveness of a reinforced asphalt overlay. The reinforcement product to be applied is much dependent on the location of the reinforcing product relative to the crack zone and the surrounding medium (asphalt or concrete) affects the effectiveness of the reinforcement products (Binh Vuong et al. 2009). Most

commercial steel products have a much higher stiffness and tensile strength than asphalt, and their thermal dimensional stability (dimensional variation because of temperature increase) is fundamental considering the high temperature of the asphalt mixture during laying. The steel dilatation could change significantly the geometry and physical properties of the reinforcement, compromising their role. In order to reduce the risk of steel dilatation, a slurry seal layer was introduced between the reinforcement and the asphalt layer.

In this research context, the aim of the paper is to evaluate the effects of four steel reinforcements in terms of pull-out resistance. To this end pull-out tests were carried out in agreement to *prescriptions techniques PTV 867 (version 0.8, 15/4/2013)*. The study was carried out in two different phases:

- phase 1: materials analysis and sample test construction using four different steel reinforcement types.
- phase 2: pull-out tests and analysis of the results.

The effects of the different steel reinforcements within the asphalt layers will be studied, analyzing the crossbars shape effects and their interaction with the asphalt layers.

2 METHODOLOGY

2.1 *Steel wire mesh reinforcements*

The research project has involved the use of steel reinforcements as reinforcement system in test samples. The steel reinforcement is composed of double twist hexagonal meshes (8 × 10 type) with crossbars intertwined with them. In this study four different types of reinforcement were analyzed, classified according to the shape of the crossbar:

- Mesh with a smooth bar (Figure 1a): bar diameter 3.9 mm and 4.4 mm;
- Mesh with one hump bar (Figure 1b): bar diameter 3.9 mm and 4.4 mm;
- Mesh with two humps bars (Figure 1c): bar diameter 3.9 mm and 4.4 mm;
- Mesh with double torsion bar (Figure 1d): torsioned flat wire.

Table 1 shows the characteristics of the steel bars.

2.2 *Sample preparation*

The procedure is based on the Belgian technical specification edited by COPRO (PTV 867 version 0.8 15/4/2013), which describes the procedure for applying steel reinforcing nettings on bituminous roads. All the samples were prepared within a wooden mould (350 × 200 × 90 mm). An asphalt base layer (40 mm) was mixed and compacted using an asphalt concrete AC 0/8 mm. The aggregates bulk density was obtained according to UNI EN 1097-6, and is equal to 2690 kg/m^3. The bitumen percentage is equal to 5.41% by aggre-

Table 1. Steel bar characteristics.

Type of Reinforcing	Bar Diameter (mm)	Minimum amount of zinc (g/m^2)	Ultimate tensile strength (kN /m)
smooth bar	3.9	275	35
	4.4	280	40
one hump bar	3.9	275	35
	4.4	280	40
two humps bar	3.9	275	35
	4.4	280	40
torsioned flat wire	–	125	32

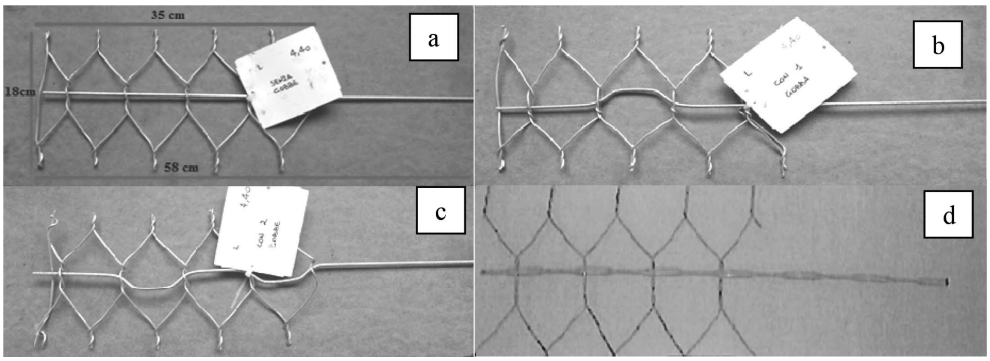

Figure 1. a) Mesh with the smooth bar. b) Mesh with one hump bar. c) Mesh with two humps bar. d) Product with torsioned flat wire.

Table 2. Asphalt mixture characteristics.

Sample	Bulk density [kg/m^3]	Residual voids [%]
1	2319	6.23
2	2320	6.17
3	2318	6.25
Average	2319	6.22

Figure 2. Application of the slurry seal.

gates weight, and 5.13% by mixture weight. The volumetric asphalt concrete characteristics are reported in Table 2.

The amount of AC used is equal to 6.2 kg and was calculated according to EN 12697-33, in order to obtain a bulk density of 2250 kg/m^3 and a layer thickness of 40 mm after compaction. The emulsion type C55B1, at a rate of 0.2 kg/m^2 of residual binder, was applied on the top of the base layer and then the steel reinforcing netting was placed. The slurry seal 0/6.3 mm at a rate of 17 kg/m^3 was laid in order to obtain 10 mm of thickness (Figure 2).

At the end the asphalt top layer (40 mm) was mixed and compacted using an asphalt concrete AC 0/12. The aggregates bulk density was obtained according to UNI EN 1097-6, and is equal to 2690 kg/m^3. The mixture bitumen percentage is equal to 5.35% by aggregates weight, and 5.07% by mixture weight. Also for the top layer, 6.2 kg of AC was weighted in order to obtain a bulk density of 2250 kg/m^3 and a layer thickness of 40 mm after compaction. The compaction of both AC layers was performed with a static compaction at the

temperature of 160°C. The samples were prepared in pairs for each type and 14 samples were made in compliance with EN 12697-33 (Figure 3).

Table 3 shows the numbering of the fourteen blocks and the type of steel reinforcing product they contain.

2.3 *Test method and procedures*

Pull-out tests were performed for the 14 samples, two for each type of reinforcing mesh, as described previously. The sample was placed inside a steel box, designed in order to confine the sample during the pull-out test (Figure 4). All specimens were at least 2 weeks old at the time of testing, allowing sufficient hardening of the slurry seal layer.

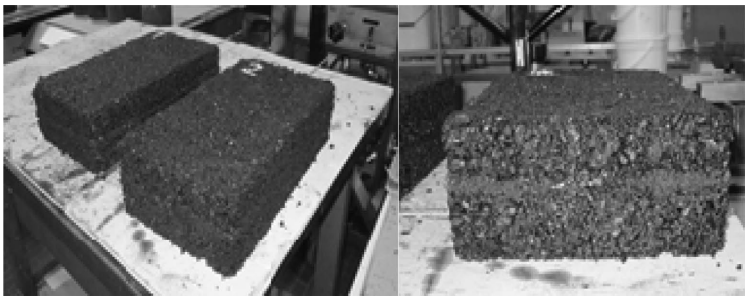

Figure 3. Finished specimens after demoulding.

Table 3. Overview of the test specimens.

Type of reinforcement	Bar code	Bar diameter (mm)
smooth bar	RM A1	3.9
	RM B1	
	RM C1	4.4
	RM D1	
one hump bar	RM A2	3.9
	RM B2	
	RM C2	4.4
	RM D2	
two humps bar	RM A3	3.9
	RM B3	
	RM C3	4.4
	RM D3	
torsioned flat wire	A	–
	B	

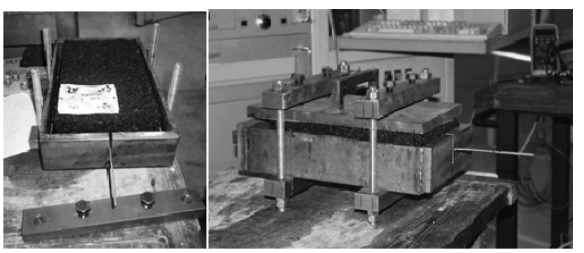

Figure 4. Steel box.

The tests were performed on a tensile test device at room temperature in the displacement controlled mode, with a displacement rate of 1 mm/min. A preload of 200 N was applied. The tests were stopped at a displacement of 30 mm (Figure 5). The confinement pressure of 0.1 N/mm^2 was distributed over the specimen faces. To obtain the required pressure a torque wrench was used, considering a vertical force of 1750 N acting on each bolt. The applied moment was determined with the following formula:

$$M = k\ d\ F_{p,cd,} \tag{1}$$

where $F_{p,cd}$ = 1750 N (vertical force on each bolt), k = 0.13 (factor depends on the type of bolt), d = 520 mm (length of the torque wrench). The torque moment applied for each bolt was equal to 120 Nm.

2.4 *Data analysis*

It will be evaluated whether the following two criteria, given in the Belgian technical specification edited by COPRO (PTV 867 version 0.8 15/4/2013), are satisfied:

- Criterion 1: requires that the average maximum tensile force (N) of each sample is greater than 2000 N.
- Criterion 2: requires that the average slope (N/mm) of the linear interpolation, evaluated from 1 to 3 mm, is greater than 200 N/mm.

3 RESULTS AND DISCUSSION

3.1 *Criterion 1*

Figure 6 shows the force versus displacement curves of the fourteen pull-out tests. Figure 8 shows the same data in the range up to 2 mm. From the force-displacement curves, the behavior of the samples was analyzed related to the shape and diameter of the bar reinforcement. The smooth bars force-displacement curves (RM A1, RM B1, RM C1 and RM D1) show the maximum tensile force at rather small displacement (0.93 and 0.52 mm). In particular, RM A1 and RM B1 reached a maximum force of 2346.1 N and 1917.2 N, respectively, and the average value of the two tests (2140.63 N) complies with the first criterion.

Figure 5. Tensile test device.

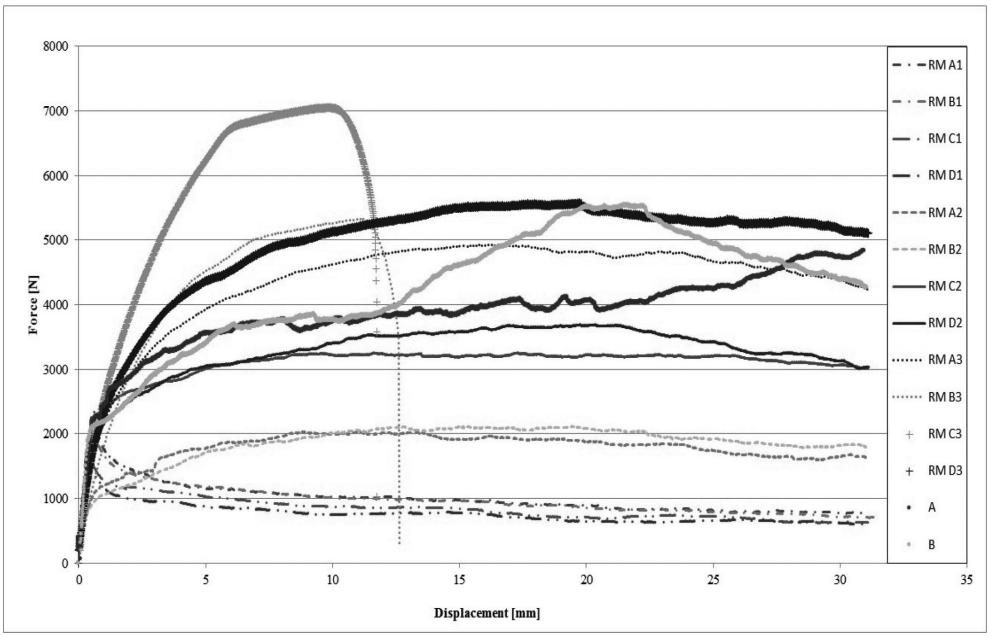

Figure 6. Overview of all tests.

Table 4. Maximum force and displacement at maximum force.

Type of reinforcing	Bar diameter (mm)	Bar Code	Maximum force (N)	Mean maximum force (N)	Displacement at maximum force (mm)	Mean value (mm)
smooth bar	3.9	RM A1	2364.1	2140	1.00	0.93
		RM B1	1917.2		0.86	
smooth bar	4.4	RM C1	1833.4	1681	0.57	0.52
		RM D1	1530.2		0.48	
one hump bar	3.9	RM A2	2038.9	2079	11.00	13.00
		RM B2	2120.4		15.00	
one hump bar	4.4	RM C2	3256.5	3474	17.40	18.70
		RM D2	3692.8		20.00	
two humps bar	3.9	RM A3	4933.6	5134	16.10	13.60
		RM B3	5335.6*		11.11*	
two humps bar	4.4	RM C3	7058.3*	6319	9.80*	14.76
		RM D3	5581.4		19.72	
torsioned flat wire	–	A	4856.2	5202	30.00	25.80
		B	5549.0		21.60	

Table 4 shows the maximum force and the displacement at maximum force for each specimen.

On the contrary, the RM C1 and the RM D1 maximum forces did not satisfy the first criterion. This result is related to the sample curing which in this case was less than two weeks. Therefore, the curing time of the slurry seal layer can affect the test results in terms of maximum force reached. Figure 6 shows that the samples with one hump bar (RM A2, RM B2, RM C2 and RM D2) reached a maximum tensile strength value at a much higher displace-

ment than the samples with smooth bars. In particular, the force-displacement curves of RM A2 and RM B2 reached an average maximum force of 2079.2 N at an average displacement of 13 mm. The RM C2 and RM D2 bars exhibit a higher tensile strength than the bars having the same shape but a smaller diameter. In this case, the average maximum force registered was close to 3500 N at an average displacement of 18 mm. The results are strongly influenced by the size of the bar, in particular, the 4.4 mm bar diameter experiences more friction between the bar and the slurry seal and consequently has a higher pull-out resistance. The one hump bars 4.4 mm and 3.9 mm both satisfy the first criterion. As shown in Figure 6 the RM A3 force-displacement curve has a maximum force value of 4933.6 N. After the maximum, the force decreased but the level remained high throughout the test and was still above 4.5 kN at the end of the test. The bar shape with two humps has substantially influenced the test results; the load was transferred on the wire mesh reinforcement that has dissipated the energy transmitted to the tensile device. For the RM B3, the force-displacement starts from zero and reaches the maximum value of 5332 N quickly. At this point the reinforcing bar was broken and the test was interrupted. The same phenomenon occurred for the RM C3 at 7058.3 N. On these specimens, the hump placed on the outer boundary was exposed to the steel box, generating a confinement that has broken the bars (Figure 7).

Out of the fourteen specimens studied, the RM D3 sample has reached the maximum tensile force peak. In this case, the position of the two humps and the 4.4 mm bar diameter have guaranteed a high pull-out resistance. For the two humps bar the first criterion is always satisfied. Making a comparison between RM A3 and RM D3, it follows that the latter reaches higher values since it has a larger diameter. For the double torsion bars, A and B, the force–displacement curves have reached the mean maximum force value of 5.2 kN. This value, similar to the value reached by the two humps bar of RM 3.9 mm, was lower than the peak tensile force reached by the two humps bars RM 4.4 mm.

3.2 *Criterion 2*

Through the second criterion the cross reinforcement anchoring degree is rated by checking the slope obtained from the pull-out curves between 1 mm and 3 mm. As described above, for the criterion to be satisfied the average slope value must be greater than 200 N/mm.

In Table 5 the slope values of the 14 specimens are reported. For the samples with smooth bar the mean slope values are negative and equal to –186.76 N/mm for RM A1 and RM B1, and –66.72 N/mm for RM C1 and RM D1. The negative parameters depend on the smooth bar tensile behavior. As seen in the previous paragraph, these specimens reached the maximum force at a displacement less than 1 mm and in the next log lost strength; therefore, the curve trend in the 1–3 mm displacement range is decreasing.

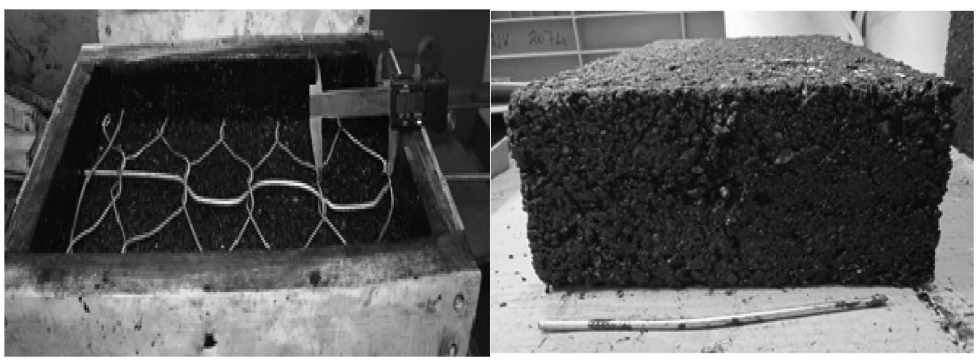

Figure 7. Breaking of the sample due to the steel box confinement.

Table 5. Slope values in 1–3 mm displacement range.

Type of Reinforcing	Bar Diameter (mm)	Bar Code	Slope (N/mm)	Mean Value (N/mm)
smooth bar	3.9	RM A1	–198.6	–186.70
		RM B1	–174.9	
smooth bar	4.4	RM C1	–50.0	–66.72
		RM D1	–83.3	
one hump bar	3.9	RM A2	118.9	135.89
		RM B2	152.8	
one hump bar	4.4	RM C2	192.8	234.43
		RM D2	276.0	
two humps bar	3.9	RM A3	571.9	722.35
		RM B3	872.7	
two humps bar	4.4	RM C3	1116.3	891.78
		RM D3	667.3	
torsioned flat wire	–	A	332.93	354.01
		B	375.1	

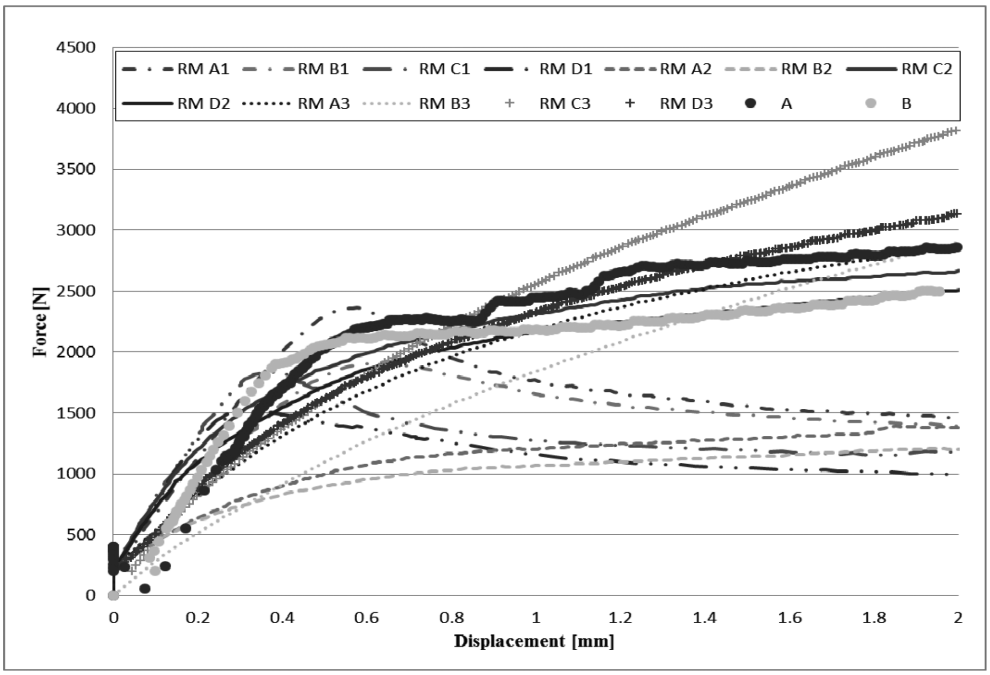

Figure 8. Overview of all tests in the range from 0 to 2 mm.

The one hump bars have satisfied the second criterion only for RM 4.4 mm (234.43 N/mm). Also for this criterion the highest values were obtained in tests conducted on the bars with two humps. In particular, for the 3.9 mm types (RM A3 and RM B3) a mean value of the slope equal to 722.35 N/mm has been obtained (Figure 9); for the LBG types (RM C3, RM D3) a mean value of 891.78 N/mm has been found (Figure 9). Therefore both types with two humps have satisfied the second criterion. The curves extrapolated from tests on double torsion bars have reached a mean value of 354 N/mm; also in this case the second criterion is

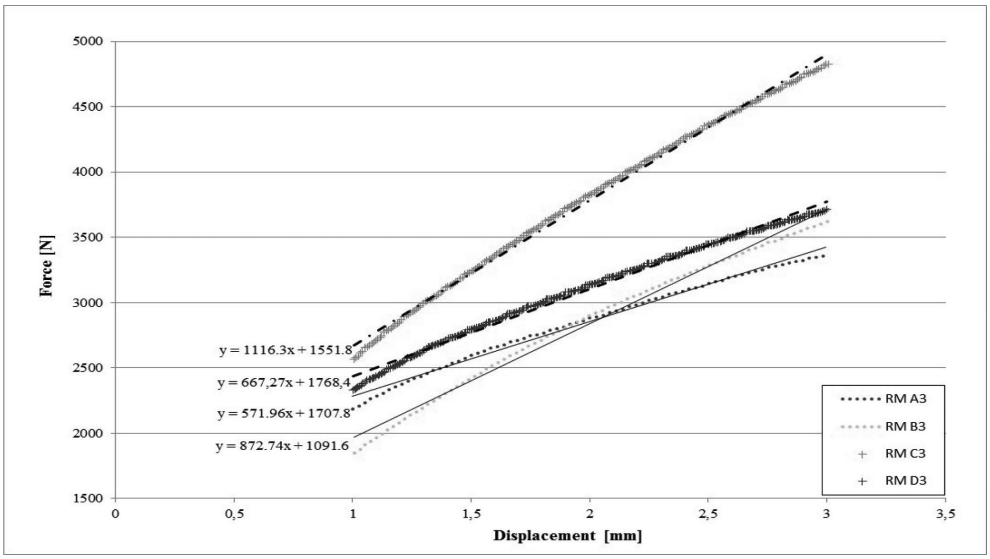

Figure 9. RM A3, RM B3, RM C3, RM D3 pull–out curve in 1–3 mm displacement range.

met, however, the values obtained are considerably lower compared to the bars with 2 humps of the type RM A3, RM B3, RM C3 and RM D3.

4 CONCLUSIONS

The main objective of this research was to study how the different types of transversal bars in steel reinforcements react to a pull-out test and therefore their influence on the pavement structure behavior. Based upon this research, the following concluding remarks can be made:

- The good quality of the Slurry Seal has a significant role in terms of protection of the steel geogrid at high temperatures and in terms of increasing the adhesion between the bars and the pavement structure. Therefore, the friction between the slurry seal layer and the steel reinforcement confers greater resistance to the system.
- The stress-strain response of the system is closely related to the different types of bars in terms of both shape and diameter. An increase of the number of humps and the diameter of the bars results in a higher maximum tensile force reached; the same factors also do increase the anchor level.
- The curing time of the asphalt samples is relevant; bitumen oxidation, and consequently its stiffening, supports the interaction between the steel bars and the asphalt concrete.

Based on the analysis of the results, the samples with two humps bars have exhibited the best performance in terms of tensile resistance and anchorage. Finally it can be stated that the reinforcement performance, especially for those with one and two humps, may depend on their installation and position. The humps must not be installed on the outer boundary of the road to avoid shear failure of the bar. At the end, a surface layer of minimum 40 mm bituminous mixture must be laid in order to guarantee the superstructure performance.

ACKNOWLEDGEMENTS

The authors take this opportunity to thank Eng. Marco Vicari and the Maccaferri Group for the considerable help they gave us in carrying out the tests.

REFERENCES

Said S.F., Carlsson H., Hakim H. 2009. Performance of flexible pavements reinforced with steel fabric. Bearing Capacity of Roads, Railways and Airfields 1: 1133–1141.

Xiaochao T., Ghassan R.C. and Angelica Palomino A., 2008. Evaluation of geogrids for stabilising weak pavement subgrade. *International Journal of Pavement Engineering* 9: 413–429.

Tataranni P., Sangiorgi C., Simone A., Vignali V., Viola P. and Dondi G. 2015. Effects on bonding of anti-reflective cracking solutions at the top bituminous interface of a small airport pavement: a laboratory and modeling study. 8th RILEM Symposium on testing and characterization of sustainable and innovative bituminous materials, October 7–9, Ancona, Italy.

Dondi G., Simone A., Vignali V. and Manganelli G. 2012. Numerical and experimental study of granular mixes for asphalts. *Powder Technology* 232: 31–40.

Dondi G., Vignali V., Pettinari M., Mazzotta F., Simone A. and Sangiorgi C. 2014. Modeling the DSR complex shear modulus of asphalt binder using 3D discrete element approach. *Construction & Building Materials* 54: 236–246.

Dondi G., Simone A., Vignali V. and Manganelli G. 2012. Discrete element modelling of influences of grain shape and angularity on performance of granular mixes for asphalts. *Procedia - Social & Behavioral Sciences* 53: 399–409.

Dondi G., Simone A., Vignali V. and Manganelli G. 2012. Discrete particle element analysis of aggregate interaction in granular mixes for asphalt: combined DEM and experimental study. Proceedings of 7th RILEM International Conference on Cracking in Pavements, June 20–22, Delft, The Netherlands, ISBN 978-94-007-4565-0.

Namir G.A., Saad F.I., Nabil H.J. 2013. Experimental Study On Surface Steel-Reinforcement For Asphalt Pavements. Journal of Engineering and Development 17: 110–127.

Baek, J. and Al-Qadi I.L. 2006. Effectiveness of Steel Reinforcing Interlayer Systems on Delaying Reflective Cracking, Proceedings of Airfield and Highway Pavement: Meeting Today's Challenges with Emerging Technologies, ASCE Atlanta, United States.

Vicari M. 2007,"Reinforcement with Double Twist Steel Wire Mesh: Modeling and Laboratory Experiences to Evaluate the Design Life Improvement of Asphalt Pavements, 4th International SIIV Conference, Palermo, Italy.

De Bondt, A.H. and Scarpas A. 2006. Design of reinforced overlays. 85th Annual Meeting TRB, Washington, D.C., United States.

Vuong B., Choi X., Hoque Z. 2009 Assessment of reinforced asphalt products for road applications using finite element modelling. Proceedings of the Thirteenth International Flexible Pavements Conference, Surfers Paradise, Queensland, Australia.

Prescriptions techniques, PTV version 08, 867. Treillis d'armature en acier, 2013.